remote sensing

Article

Potential of L- and C- Bands Polarimetric SAR Data for Monitoring Soil Moisture over Forested Sites

Ramata Magagi [1], Safa Jammali [2], Kalifa Goïta [1], Hongquan Wang [1,*] and Andreas Colliander [3]

[1] Centre d'Applications et de Recherches en Télédétection (CARTEL), Université de Sherbrooke, 2500 Boul. de l'Université, Sherbrooke, QC J1K2R1, Canada
[2] Département d'Informatique, Université de Sherbrooke, 2500 Boul. de l'Université, Sherbrooke, QC J1K2R1, Canada
[3] Jet Propulsion Laboratory, California Institute of Technology, 4800 Oak Grove Drive, Pasadena, CA 91109, USA
* Correspondence: hongquan.wang@usherbrooke.ca

Abstract: This study investigates the potential of L- and C- bands Polarimetric Synthetic Aperture Radar (PolSAR) data to monitor soil moisture over the forested sites of SMAP Validation Experiment 2012 (SMAPVEX12). The optimal backscattering coefficients and polarimetric parameters to characterize the soil moisture were determined based on L-band Uninhabited Aerial Vehicle Synthetic Aperture Radar (UAVSAR), C-band RADARSAT-2, and ground measurements composed of soil and vegetation parameters collected during SMAPVEX12. Linear and circular backscattering coefficients (σ^0) and polarimetric parameters such as correlation coefficients (ρ_{HHVV}) and phase difference (φ_{HHVV}) between HH and VV, pedestal height (PH), entropy (H), anisotropy (A), α angle, surface (Ps), and double bounce (Pd) powers were used to develop the relationships with soil moisture. The analysis of these relationships shows that over the forested sites of SMAPVEX12: (a) at L-band several optimal backscattering coefficients and polarimetric parameters allow the monitoring of soil moisture, particularly the linear and circular σ^0 (r = 0.60–0.96), Ps (r = 0.59–0.84), Pd (r = 0.60–0.82), ρ_{HHHV}_30°, ρ_{VVHV}_30°, φ_{HHHV}_30° and φ_{HHVV}_30° (r = 0.56–0.81). However, compared to the results obtained with σ^0, there is no added value of the polarimetric parameters for soil moisture retrievals. (b) at C-band, only a few polarimetric parameters φ_{HHHV}, φ_{VVHV}, and φ_{HHVV} are correlated with soil moisture (r = ~0.90). They can contribute to soil moisture retrievals over forested sites when L-band data are not available.

Keywords: SAR; L-band; C-band; polarimetry; soil moisture; forested sites; SMAPVEX12

check for updates

Citation: Magagi, R.; Jammali, S.; Goïta, K.; Wang, H.; Colliander, A. Potential of L- and C- Bands Polarimetric SAR Data for Monitoring Soil Moisture over Forested Sites. *Remote Sens.* **2022**, *14*, 5317. https://doi.org/10.3390/rs14215317

Academic Editor: Luca Brocca

Received: 28 August 2022
Accepted: 18 October 2022
Published: 24 October 2022

1. Introduction

Soil moisture is a key parameter in environmental and hydrological processes related to runoff and evapotranspiration [1]. By controlling the distribution of precipitation between infiltration and runoff, soil moisture also influences soil erosion processes [2–4], weather, and climate events [5]. Due to these determining roles in the water cycle and global energy, soil moisture is recognized as an essential climate variable by the Global Climate Observing System [6]. Over the forest cover which represents 30% of Earth's surface, an extreme increase in soil moisture can produce paludification [7], while an extreme decrease in soil moisture can cause the risk of forest fires [8]. Therefore, the knowledge of soil moisture is very important for the protection and management of forested resources.

Due to high cost, in-situ soil moisture measurements are limited in space and time. With the launch of L-band passive microwave satellites Soil Moisture and Ocean Salinity (SMOS) in 2009 and Soil Moisture Active and Passive (SMAP) in 2015, considerable advances were made in soil moisture monitoring on a global scale. However, few results were obtained over areas covered by dense forests, as a result of their strong attenuation and scattering effects on microwave signals [9]. Based on the SMAP Validation

Experiment 2019–2021 (SMAPVEX19-21), Colliander, et al. [10] used a two-layer radiative transfer model [11] to retrieve soil moisture with RMSE of 0.047–0.057 m^3/m^3 over temperate forest sites from SMAP brightness temperature. During the summer of 2022, SMAP Validation Experiment 2022 (SMAPVEX22) and SMAPVEX 2022 in Boreal forests (SMAPVEX22-Boreal) were respectively conducted over temperate forests located in the USA and over the boreal forested sites of the Boreal Ecosystem Research and Monitoring Sites (BERMS) located in Saskatchewan (Canada). A huge amount of data (including soil moisture at organic/mineral layers, depths of these layers, tree trunk/branch moisture contents and sizes, L-band airborne and satellite remote sensing data) was collected in order to investigate new avenues in microwave remote sensing of the forest, develop microwave remote sensing applications of forest such as fires monitoring, improve and validate soil moisture retrieval algorithms over dense vegetation conditions (e.g., Vegetation Water Content—VWC > 5 kg/m^2) from SMAP and SMOS signatures [12]. The literature showed further improvement in soil moisture products by combining these passive microwave signatures with Synthetic aperture radar (SAR) [13,14]. In contrast to passive microwave, SAR is characterized by fine spatial resolution but low temporal resolutions (e.g., 24 days for RADARSAT-2). Furthermore, SAR data is more affected by surface properties such as surface roughness and vegetation, which make soil moisture estimation difficult particularly over forested areas [15,16]. For such dense vegetated areas, the radar signal's sensitivity to soil moisture decreases due to the scattering by vegetation biomass, which reduces the contribution of the soil in the measured signal [17,18]. In addition, forested areas represent a complex scattering environment [19] with several unknowns in the soil moisture estimation algorithms, such as the permittivity of tree components (trunk, branches, leaves) and soil layers. Polarimetric decomposition of P-band (long-wavelength) airborne radar data was used to estimate forest soil moisture [20]. Kurum, et al. [21] estimated soil moisture with RMSE of 0.044 m^3/m^3 for SMAP Validation Experiment 2012 (SMAPVEX12) forest sites, characterized by vegetation water content ranging from 7.3 to 25.6 kg/m^2, using L-band Uninhabited Aerial Vehicle SAR (UAVSAR) data acquired with wide ranges of incidence angles (an angle between radar beam and the normal direction of the land surface). They found that VV-polarized backscattering power provides robust retrieval results, while the inclusion of HH-polarization did not improve the retrieval. At C-band, the radar signal is affected by the structure and the water content of vegetation. The degree of interaction with the vegetation depends on the incidence angle and the polarization [22].

Over forested areas, most of the research works have focused on the estimation of biomass [23] and few investigations have attempted to estimate soil moisture in boreal forests [24,25]. The obtained results were sites specific and were limited by the use of single-polarization C-band SAR such as ERS-1 and RADARSAT-1. To reduce the influence of vegetation on the radar signal and thus for a better access to soil parameters, a low incidence angle (<30°) or low frequency (L-band) can be used [22,26]. With fully polarimetric SAR (PolSAR) data, several investigations focused on target classification using polarimetric discriminators [27,28] and target decomposition approaches [22,29–31]. Despite the additional information provided by the PolSAR data on the structural change of vegetation and surface roughness as well as on the scattering contributions of these parameters [17,18,32], it is a great challenge to estimate soil moisture from polarimetric parameters. Studies found in the literature were primarily focused on burned forest areas with low biomass [17,18].

This paper aims to analyze the potential of L- and C- bands fully PolSAR signatures for monitoring soil moisture over the SMAPVEX12 forested sites. During the SMAPVEX12 campaign, soil (soil moisture, roughness) and vegetation (Diameter at Breast Height—DBH of trees and floor cover) parameters were collected over four forested sites along with L-band UAVSAR data at 25–65° incidence angles and C-band RADARSAT-2 data. In this paper, the relationships between L- and C- bands SAR parameters and soil moisture were first developed. They were interpreted using statistical analyses (linear correlation coefficient and significance test) to identify the optimal backscattering coefficients and polarimetric parameters for soil moisture monitoring over forested sites. The added value of the polarimetric parameters for soil moisture retrieval was also discussed. The results obtained will be of great interest in using the recently collected SMAPVEX (SMAPVEX19-21, SMAPVEX22, SMAPVEX22-Boreal) datasets to develop improved soil moisture retrieval algorithms for forest sites. This paper is organized as follows: Section 2 presents a brief review of backscattering coefficients and polarimetric parameters which have the potential to characterize forest soil moisture, followed by the study site and the dataset description in Section 3. The methodology and the results are presented in Sections 4 and 5, respectively. Finally, Section 6 provides the conclusion.

2. SAR Scattering Parameters

In radar remote sensing, the strength of the scattering mechanisms (surface, volume, double-bounce) can be evaluated from the backscattering coefficients and polarimetric parameters (Table 1) which are extracted from the covariance and or the coherency matrices [32]. The knowledge of the predominant scattering mechanism is useful to assess the potential of the signal for retrieving soil or vegetation parameters [33]. The linear (σ^0_{HH}, σ^0_{VV}, and σ^0_{HV}) and circular (σ^0_{RR}, σ^0_{LL}, and σ^0_{RL}) are considered in this paper due to their relative potential for soil moisture monitoring highlighted by previous studies [1,14,15,34,35]. As for the polarimetric parameters, the focus is on the correlation coefficient between two channels through its amplitude (ρ) and its phase (φ), the parameters extracted from the target decompositions of Cloude-Pottier (entropy H, angle α, anisotropy A) and Freeman-Durden (surface and dihedral scattering powers Ps and Pd, respectively) and the pedestal height. Table 1 presents the list of backscattering coefficients and polarimetric parameters used in this study.

Table 1. Backscattering coefficients and selected polarimetric parameters.

Backscattering Coefficients		Selected Polarimetric Parameters	
σ^0_{HH}, σ^0_{VV}, σ^0_{HV}	Backscattering coefficients (dB) in linear polarizations HH, VV, and HV	φ_{HHVV}, φ_{HHHV}, φ_{VVHV}	Phase differences between two channels HH-VV, HH-HV, and VV-HV
σ^0_{RR}, σ^0_{LL}, σ^0_{RL}	Backscattering coefficients (dB) in circular polarizations RR, LL, and RL	ρ_{HHVV}, ρ_{HHHV}, ρ_{VVHV}	Correlation coefficients between two channels HH-VV, HH-HV, and VV-HV
		PH	Pedestal height
		H, A, α	Entropy, Anisotropy, alpha
		P_s, P_d	Surface and volume scattering powers (dB)

2.1. Backscattering Coefficients

The sensitivity of the backscattering coefficient to the target characteristics is highly dependent on the amount of these characteristics, particularly that of the moisture content, biomass and the geometrical structure (roughness, vegetation architecture such as scatterer size and orientation) as well as on the sensor frequency, polarization, and incidence angles [34]. Indeed, a study conducted with ERS-1 (C-band, VV polarization, 23°) and JERS-1 (L-band, HH polarization, 35°) showed that the sensitivity of the backscattering coefficient to biomass is influenced by soil moisture [35]. Several studies pointed out that at C-band SAR signature comes mainly from the upper layer of trees and it quickly saturates with vegetation density [33]. In contrast, at lower frequencies (L- and P-bands), the vegetation effect is less important (less attenuation and more penetration in the vegetation cover), so that they allow better monitoring of soil moisture.

In this context airborne data (AIRSAR, UAVSAR) collected in the framework of several research programs played a significant role in the understanding of low-frequency SAR data and the development of soil moisture retrieval algorithms over forested sites. Using P-band AIRSAR data collected over tropical forests, Truong-Loï, et al. [36] developed analytical formulations of σ^0_{HH}, σ^0_{VV}, and σ^0_{HV} to estimate soil moisture, soil roughness and vegetation biomass. For soil moisture retrieval, they obtained an RMSE less than 4 (%vol.) which increased with the sensor incidence angle. In a study conducted with AIRSAR data collected over the Boreal Ecosystem-Atmosphere Study (BOREAS) forest [37], the double-bounce of old jack pine (OJP) site is found to be predominant for L- and P-bands horizontal polarization (L-HH and P-HH) and P-band vertical polarization (P-VV). Based on these results, soil moisture was retrieved over the OJP site from parametric models developed for only the double-bounce scattering [33]. Using L-band UAVSAR data and a forward scattering model, Tabatabaeenejad, et al. [26] investigated the soil moisture retrieval over the forest sites of the CanEx-SM10 experiment [38]. In accordance with Moghaddam, et al. [33], they found a good potential of L-band radar to retrieve soil moisture under forests, such as the abovementioned OJP site and the young jack pine (YJP) site with trunk-ground double-bounce as a predominant scattering mechanism. On the contrary, large retrieval errors were obtained over the old black spruce site, characterized by a complex forest floor (understory, moss) which can attenuate the soil scattering mechanisms containing the soil moisture information [39]. While most of the soil moisture investigations conducted with low-frequency SAR over forested sites used airborne data, at the satellite scale the focus is generally on the biomass estimation from higher frequencies. Bourgeau-Chavez, et al. [18] conducted a rare sensitivity study of C-band SAR data to soil moisture under forested sites. They obtained a correlation of about 0.68–0.78 between the soil moisture and the RADARSAT-2 HH, VV, and HV polarization signals acquired at 19–21° incidence angle over burned boreal forest sites (shrub, sparse, and moderately dense) in Alaska. To discriminate between dry and wet soil conditions, a study conducted over forested sites with biomass varying from low to high showed the great potential of RADARSAT-2 HH and LR polarizations [18].

2.2. Polarimetric Parameters

Soil moisture estimation from polarimetric parameters is relatively recent [40–44]. Similar to the use of backscattering coefficients, high vegetation amount negatively impacts the algorithm accuracies [43]. However, over forested areas characterized by high biomass and complex scattering environments, the investigations using polarimetric parameters for soil moisture retrieval are limited. Since the polarimetric decomposition provides the strength of individual scattering mechanisms, the decomposition parameters related to the dominant surface or double-bounce scattering could be used for soil moisture estimation. Without focusing on the theoretical aspects of the polarimetric parameters listed in Table 1, Sections 2.2.1–2.2.3 briefly present the results of previous investigations about the contribution of the correlation coefficient (amplitude and phase), the pedestal height, and the parameters of two polarimetric decompositions (Freeman-Durden and Cloude-Pottier) to soil moisture retrieval.

2.2.1. Amplitude and Phase of the Correlation Coefficient

The amplitude of the correlation coefficient between two channels indicates the degree of correlation of these channels while its phase measures their phase difference. Using the P-band airborne polarimetric data of NASA/JPL data, Le Toan, et al. [45] showed that the amplitude and the phase of the correlation coefficient between HH and VV polarizations (ρ_{HHVV} and φ_{HHVV}) can be used for the biomass estimation over the Landes pine forest, in France. No attempt was made by Le Toan, et al. [45] for soil moisture estimation. Compared to the backscattering coefficients acquired over bare soils at P-, L-, and C- bands, Borgeaud and Noll [46] showed the supplementary information contained in ρ_{HHVV} and φ_{HHVV} for the retrieval of geophysical parameters. Later, Skriver, et al. [47] showed that at L- and C-bands, both the magnitude and the behavior (angular and temporal) of ρ_{HHVV} and φ_{HHVV} are related to the scattering mechanisms of crops. Indeed, for a surface scattering ρ_{HHVV} is high with a value close to 1 (it is smaller for volume scattering) while small values near 0° are found for φ_{HHVV} [46–48]. Mitigated results were obtained about the sensitivity of ρ_{HHVV} to soil roughness [46,49], while several studies showed that ρ_{HHVV} and φ_{HHVV} are not sensitive to soil moisture [50]. Over low biomass boreal forested sites, no correlation was obtained at C-band between φ_{HHVV} and the soil moisture [17].

2.2.2. Pedestal Height

The pedestal height can be used as an indicator of non-polarized signals [28]. Low pedestal height expresses a polarized signal; and conversely, high pedestal height characterizes a depolarized signal due to volume scattering [47]. Therefore, the low pedestal height values which are characteristic of the surface scattering mechanism can be used for soil moisture monitoring. Over bare soil, Sokol, et al. [1] obtained a good correlation (r = 0.82) between the pedestal height and the soil moisture. This correlation value decreases to 0.74 and 0.61, over burned and unburned boreal forested sites, respectively [17]. However, the increasing relationship between the pedestal height and the surface roughness found in McNairn, et al. [48] will affect the observed correlations between the soil moisture and the pedestal height.

2.2.3. Polarimetric Decomposition Parameters

The two widely used decompositions are the model-based decomposition of Freeman-Durden and the eigenvectors/eigenvalues decomposition of Cloude-Pottier [22,29]. They allow us to evaluate three scattering mechanisms [44,51] which can be used individually or together for the monitoring of the surface parameter(s) of interest [43,51,52].Considering the soil moisture estimation, these two decompositions approaches were seldom used over forested areas [17,18].

Freeman-Durden decomposition [22]: It partitions the signal into a surface (Ps), a volume (Pv), and a double bounce (Pd) scattering. The first and the second components come from the ground surface and the vegetation, respectively. The third one resulted from the interaction between the ground surface and the vegetation [22]. Based on the rationale of Freeman-Durden decomposition, other model-based decompositions have been developed by considering the scattering mechanisms in different ways [31,40,53]. Due to the complementarity between the soil moisture inversion results obtained from Ps and Pd, the main advantage of the simultaneous use of Ps and Pd is the increase of the retrieval rate [40]. Using low incidence angle (19–21°) RADARSAT-2 data, Bourgeau-Chavez, et al. [18] and Bourgeau-Chavez, et al. [17] showed the potential of Ps and Pd to monitor the soil moisture over low biomass boreal forested sites. However, a study conducted over a tropical forest with L-band high incidence angles (63–70°) airborne data showed a good correlation (r = 0.63) between Pd and the stem volume [54]. Through a model-based polarimetric decomposition adapted for the first time to P-band airborne data, Jagdhuber, et al. [20] used the dominant scattering component between Ps and Pd to estimate soil moisture over forest sites.

Cloude-Pottier decomposition [29]: It provides three relevant polarimetric parameters which are the entropy (H), the anisotropy (A), and the alpha angle (α). They were widely used to distinguish the scattering mechanisms involved in a given signal [43,49]. Furthermore, Cloude-Pottier decomposition is used for soil moisture retrieval over bare soils [52,53] or to improve soil moisture retrieval over vegetated areas [31,55]. It was shown by Baghdadi, et al. [41] that the alpha angle (α_1) associated with the first eigenvector can be used for the detection of very wet soils (>0.3 m^3/m^3). Nevertheless, the weak correlation observed at C-band between H, α, and soil moisture shows that the sensitivity of these polarimetric parameters to soil moisture is not clear. Over low biomass boreal forested sites, Bourgeau-Chavez, et al. [18] found low correlations between the soil moisture and the parameters H, A, and α.

The limitations of the C-band backscattering coefficient for soil moisture retrieval are presented in Section 2.1. In the present paper, we analyzed the added-value of C-band polarimetric parameters to estimate soil moisture over SMAPVEX12 forested sites which are different from tree and floor characteristics. Similar analyses are conducted at L-band in order to determine the optimal PolSAR parameters (backscattering coefficients, polarimetric parameters) or a set of optimal PolSAR parameters for that topic. Investigations which are close to ours are those of Bourgeau Chavez et al. [14,15] with however two main differences: (1) we conducted at two frequencies (instead of one frequency) sensitivity studies of backscattering coefficients and polarimetric parameters to soil moisture over forested sites; (2) these sites are characterized by different floor characteristics and biomass varying from low to high (instead of low biomass forested sites only).

3. Study Area

This study focused on the forested sites of the SMAPVEX12 campaign ([56], https://smapvex12.espaceweb.usherbrooke.ca (accessed on 17 October 2022)) which took place in the southwest of Winnipeg (98°0′23″W, 49°40′48″N), Manitoba in Canada during the summer of 2012. Figure 1 delineates the location (red rectangles) of four forested sampling sites, namely F1, F2, F3, and F5, which are dominated by forest/grassland with the Trempling Aspen as the main tree species. The area is flat with an elevation of about 315 m (http://fr-ca.topographic-map.com/places/Manitoba-437295/ (accessed on 17 October 2022)). The annual precipitation is around 520 mm (https://weather-and-climate.com/) (accessed on 17 October 2022).

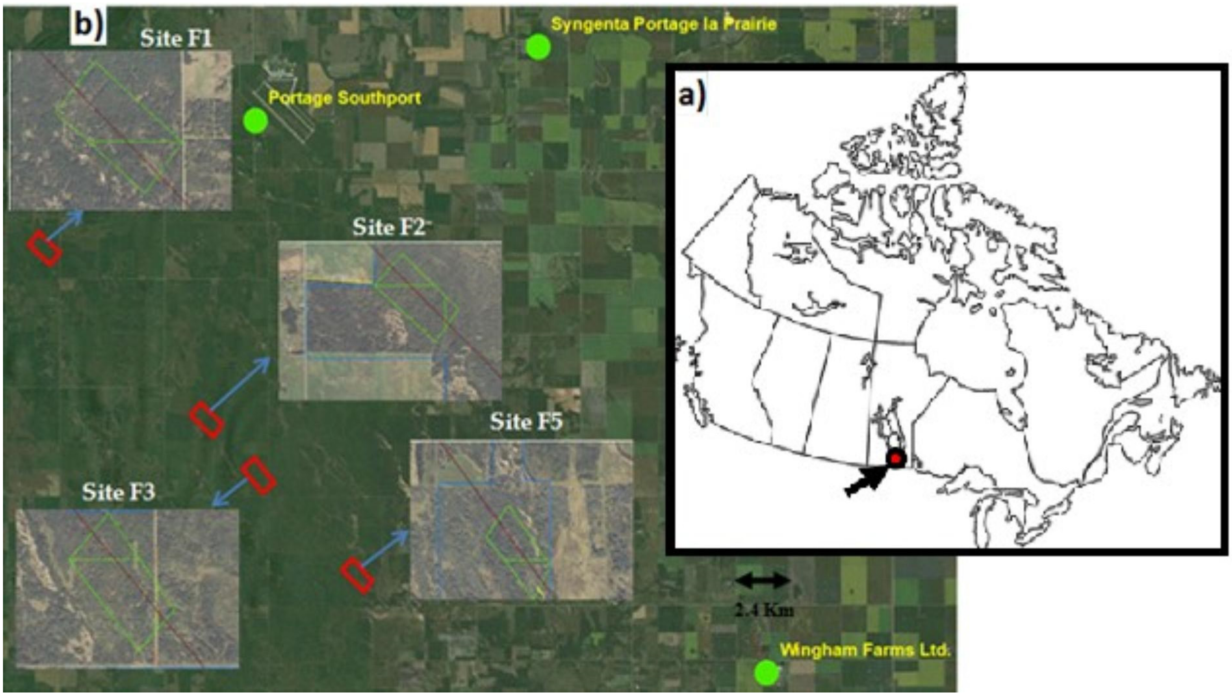

Figure 1. Location of (**a**) SMAPVEX12 area and (**b**) four forested sampling sites of SMAPVEX12.

4. Data

The SMAPVEX12 experiment was conducted for 6 weeks between 6 June and 17 July 2012, to capture variable soil and vegetation conditions. More details about SMAPVEX12 data collection can be found in [56]. The data consisted of ground measurements of soil and vegetation characteristics, satellite and airborne SAR, and auxiliary data.

4.1. Ground Measurements and Processing

For each forested site which is approximately 800 m × 800 m, a random circular area of 200 m diameter was selected. Within this area, measurements characterizing soil (soil moisture and surface roughness) and vegetation (diameter at breast height-DBH, water content, density of the trunk, cover floor) were collected.

Soil moisture: Volumetric soil moisture was manually measured with Hydra probe sensors. In addition, we make use of 5 cm depth hourly soil moisture measurements collected by temporary stations installed over the sites F1, F2, and F3 by Manitoba Agriculture, Food and Rural Initiatives (MAFRI) and the United States Department of Agriculture (USDA). Over the F1 site, the manually measured soil moisture values were lower than the soil moisture measured by the USDA station. Also, due to the high amount of organic matter covering the soils of the forested sites, issues of calibration occurred with the manual soil moisture measurements. Therefore, measurements by temporary stations will be considered for the F1, F2, and F3 sites. Since no station has been installed over the F5 site, the manually measured soil moisture will be considered for this site. For each date, soil moisture values taken between 6:30 am to 12 am were averaged. Figure 2 presents the temporal evolution of soil moisture measurements along with precipitation over F1, F2, F3, and F5 sites. It shows that for the four sites, soil moisture goes relatively through three phases according to precipitation. It is high from 7 June (DOY 159) to 22 June (DOY 174) 2012 and then decreases from 6 June (DOY 158) to 12 July (DOY 164) 2012 due to the lack of precipitation. At the end of the field campaign, it increases with some rain events.

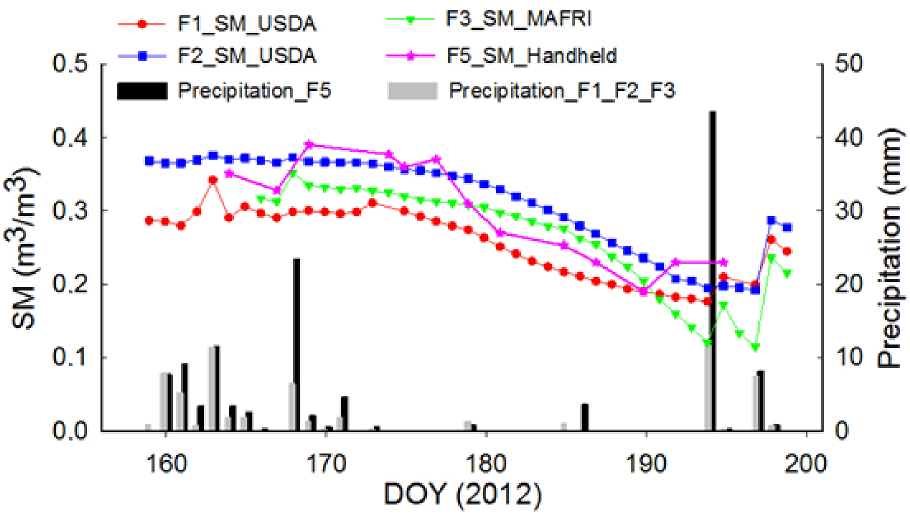

Figure 2. Temporal profile of soil moisture and precipitation over F1, F2, F3, and F5 forest sites.

Surface roughness: Soil surface roughness parameters (rms height, correlation length) were measured at two locations over the F1, F2, and F3 sites and at one location over the F5 site in the look directions of RADARSAT-2 and UAVSAR sensors. For each location and each look direction, the measurements result from a 3-m profile obtained by combining three measurements of a 1-m long pin profilometer with a sample resolution of 0.5 cm. Table 2 shows the average values of the surface rms height and correlation length obtained over each forested site. The values of rms and correlation length vary from 0.7 to 1.7 cm and 10.5 to 22.75 cm, respectively. Over site F2, the surface roughness expresses heterogeneity, resulting in a larger difference when observed from the RADARSAT-2 and UAVSAR look directions.

Table 2. Surface roughness measurements over SMAPVEX12 forested sites in the look direction of RADARSAT-2 and UAVSAR sensors.

Forest Site	UAVSAR		RADARSAT-2	
	RMS (cm)	Correlation Length (cm)	RMS (cm)	Correlation Length (cm)
F1	0.93	18.75	1.05	15.5
F2	1.63	22.75	1.04	10.5
F3	1.46	17	1.61	14
F5	0.85	13	0.77	15.5

Vegetation data: DBH was measured and then used to estimate the biomass of the dominant tree species (Trembling Aspen) with an error of 7.2 kg/m^2 [57]. In this calculation, only trees with DBH $\geq$ 0.02 m are considered, while those with smaller DBH are considered as floor cover. The estimated tree biomass is subsequently used to calculate the total biomass (biomass $\times$ tree trunk density). Results show that F3 is the densest site with biomass of 138.39 kg/m^2 while F1, F2, and F5 presents similar biomass values of 34.12 kg/m^2, 39.69 kg/m^2, and 37.7 kg/m^2 respectively (Table 3).

Table 3. Characteristics of forested sites.

	F1	F2	F3	F5
Forest type	The majority of species are Trembling Aspen			
DHP (m)	0.25	0.21	0.28	0.15
Tree VWC (kg/m^2)	15.39	25.63	7.34	14.10
Trunk density (nb/m^2)	0.14	0.25	0.43	0.54
Floor fractional cover (%)	Mainly grass (44)	Mixed (herbs, shrub dead wood, and litter) (49)	Grass and litter (69.5)	Grass (67)
Floor cover depth (m)	0.04	1.13	1.15	0.71
Biomass (kg/m^2)	34.12	39.69	138.39	37.7

The type of floor cover (undergrowth, litter, grasses, shrubs) and its depth are also determined. As shown in Table 3, F1 presents the lowest floor cover, with 44% of grass coverage and a depth of about 0.04 m. The floor fractional covers over F3 and F5 sites are very similar and higher than those of F1 and F2. F2 and F3 present very similar floor cover depth which is higher than those of F1 and F5.

Precipitation: The precipitation data were downloaded from the Environment Canada website (http://www.ec.gc.ca/ (accessed on 17 October 2022)). For F1, F2, and F3 sites, precipitation data were acquired from the Portage Southport station. The precipitation data used for the F5 site were acquired from the Wingham Farm station (Figure 1).

4.2. SAR Data and Processing

UAVSAR data: UAVSAR onboard NASA Gulfstream-III aircraft acquired fully polarimetric L-band (1.26 GHz) SAR data at 25–65° incidence angles, with a spatial resolution of 4.5 m $\times$ 5 m. The images were acquired from 17 June to 17 July during the SMAPVEX12 field campaign (http://uavsar.jpl.nasa.gov (accessed on 17 October 2022)). These images were acquired simultaneously with manual measurements of soil moisture. Table 4 shows the availability of UAVSAR data over the study area. To optimize the soil moisture monitoring over the forested sites, the flight lines providing the smallest incidence angles are considered. They are identified as winnip_31603 and winnip_31604 with incidence angles of 30° and 40°, respectively.

Table 4. Characteristics of UAVSAR data over the study area.

DOY 2012	Incidence Angle	DOY 2012	Incidence Angle
169	30°, 40°	187	30°, 40°
171	30°, 40°	190	30°, 40°
174	40°	192	30°, 40°
175	30°, 40°	195	30°, 40°
177	30°, 40°	196	40°
179	30°, 40°	199	30°, 40°
181	30°, 40°		

RADARSAT-2 data: The project also benefits from C-band fully polarimetric RADARSAT-2 images acquired at incidence angles between 20 and 30°. Table 5 shows the characteristics of the seven Wide Quad-Polarimetric RADARSAT-2 acquisitions during the SMAPVEX12 field campaign. Since F5 is not covered with RADARSAT-2 images on the same dates as ground soil moisture measurements, soil moisture monitoring at C-band cannot be conducted over this site. PolSARpro (version 5) and PCI Geomatica (version 2013) software were used for the processing of both UAVSAR and RADARSAT-2 images and the extraction/computation of the backscattering coefficients and polarimetric parameters through the following steps:

- Extraction of the covariance matrix (C) and coherency matrix (T);
- Applying a Boxcar filter 7 × 7 [58,59] to the images;
- Extraction and computation of the backscattering coefficients and polarimetric parameters;
- Images orthorectification using a road network map created with QuantumGIS and Orthoengine to remove geometric distortions.

Table 5. Characteristics of Wide mode Quad-pol RADARSAT-2 data. The ascending (A) and descending (D) directions correspond to the 7:10 PM and the 7:50 AM overpasses, respectively.

DOY 2012	Flight Direction	Beam Mode	Incidence Angle (°)
164	D	FQ8W	26.1–29.4
165	A	FQ10W	28.4–31.6
172	A	FQ6W	23.7–27.2
179	A	FQ2W	19.0–22.7
188	D	FQ8W	26.1–29.4
189	A	FQ10W	28.4–31.6
196	A	FQ6W	23.7–27.2

5. Methodology

Figure 3 presents the schematic diagram of the methodology. The backscattering coefficients and polarimetric parameters were extracted from the covariance matrix (C) and the coherency matrix (T). They are related to ground soil moisture measurements using linear relationships which are statistically interpreted from the correlation coefficients and the significance tests (p-value). Finally, the optimal PolSAR parameters (backscattering coefficients, polarimetric parameters) for soil moisture monitoring over the forested sites were identified based on the statistical analyses.

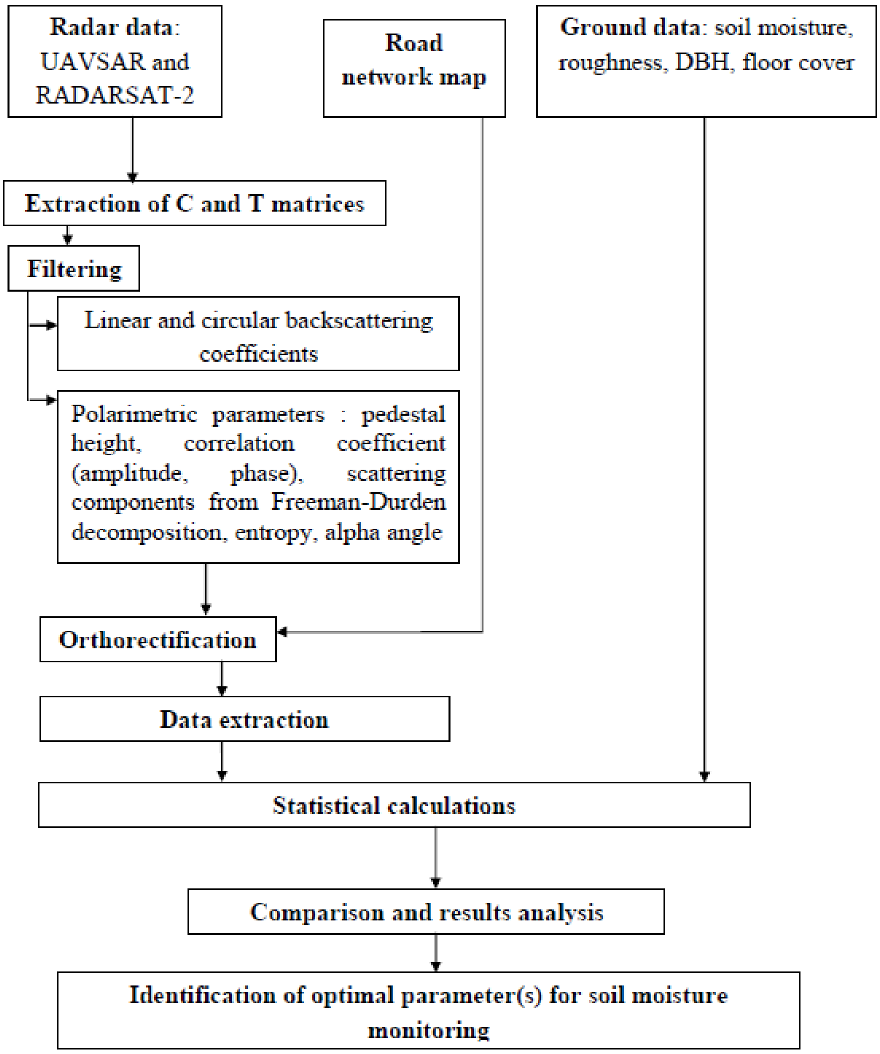

Figure 3. Schematic diagram of methodology.

5.1. Extraction of the Backscattering Coefficients and the Polarimetric Parameters

For each forest site, for each frequency, and for each SAR image acquisition date, the backscattering coefficients and the polarimetric parameters are extracted within the same polygon for which the number of pixels depends on the spatial resolution of the images (Table 6). The average values of the backscattering coefficients and the polarimetric parameters were computed over the polygons and subsequently used in this paper.

Table 6. Pixels number of each polygon for the forested sites F1, F2, F3, and F5.

	F1	F2	F3	F5
L-band images	597	596	511	715
C-band images	359	357	306	431

5.2. Linear Regressions and Statistical Analyses

For each frequency and each forested site, linear regressions were developed between ground soil moisture measurements and the mean values of the backscattering coefficients and the polarimetric parameters. These linear regressions, obtained at L- and C- bands, were interpreted for soil moisture monitoring over the forested sites using statistical analyses (linear correlation coefficient and significance test). For each regression, the correlation coefficient (r) is computed and a significance test (p-value) is conducted for statistical analyses of the regressions [17,18]. For a given risk *b*, the null hypothesis H_0 that the radar data (backscattering coefficients, polarimetric parameters) and the soil moisture are independent is tested against the alternative hypothesis H_1 that the radar data and the soil moisture are significantly correlated. If the p-value is less than *b* (here it is considered equal to 5%), the null hypothesis is rejected in favor of the alternative hypothesis and the correlation coefficient of the regression is considered statistically significant.

The magnitudes of the significant correlation coefficients were used to compare the potentials of L- and C- bands fully PolSAR data for soil moisture monitoring over forested sites with different characteristics (biomass, tree water content, floor cover, etc.). For each frequency, we determine the added value of polarimetric parameters vs. the backscattering coefficients for soil moisture monitoring over forest sites. We also identify the optimal PolSAR parameters (backscattering coefficients, polarimetric parameters) to characterize the soil moisture over the forested sites.

6. Results and Discussion

Qualitative analysis is first conducted with the temporal profiles of L- and C- bands linear and circular backscattering coefficients and those of soil moisture measurements over the least dense site F1 and the densest site F3. It is followed by the analyses of the regression results developed in Section 6.2.

6.1. Temporal Profiles of the Linear and Circular Backscattering Coefficients

6.1.1. At L-Band Using UAVSAR Data at 30 and 40°

At L-band, at 30 and 40° incidence angles, the temporal profiles of the linear and circular backscatter coefficients for all polarizations (HH, VV, HV, RR, RL, and LL) follow those of soil moisture, and particularly over F1. For both 40 and 30°, HH remains higher than VV over all the sites. Figures 4a and 5a showed that the difference between HH and VV decreases with an increase in vegetation from F1 to F3 sites. This is mainly due to the depolarization process which occurs with an increasing volume scattering. While the signals of linear polarizations are well contrasted $\left(\sigma^0_{HH} > \sigma^0_{VV} > \sigma^0_{HV}\right)$, the signals of circular polarizations are close to each other (Figures 4 and 5). For F1 and F3 sites, there is almost no difference between the 30 and 40° linear and circular backscattering coefficients. For this reason, L-band parameters will be subsequently analyzed at only 30°.

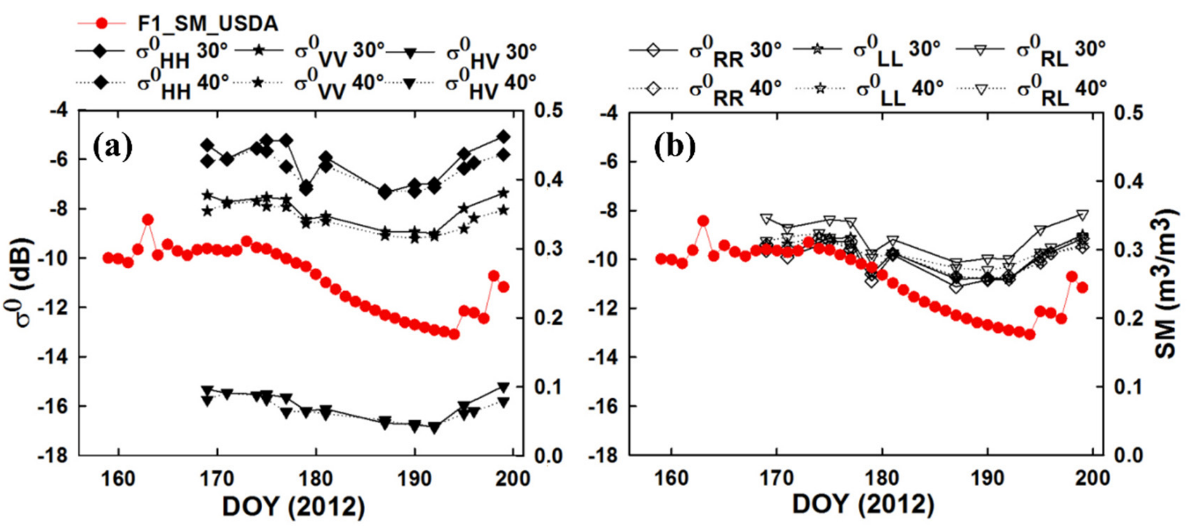

Figure 4. Temporal profiles of L-band (**a**) linear (HH, VV, and HV) and (**b**) circular (RR, LL, and RL) polarizations at θ = 30 and 40° along with soil moisture measurements over F1. F1_SM_USDA is the soil moisture measured by the USDA station.

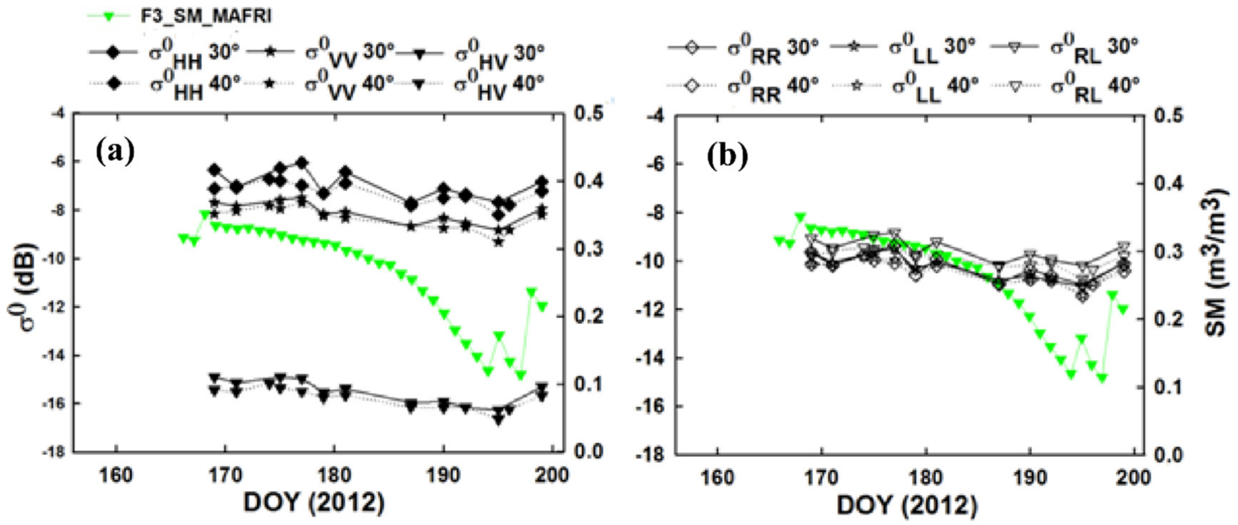

Figure 5. Temporal profiles of L-band (**a**) linear (HH, VV, and HV) and (**b**) circular (RR, LL, and RL) polarizations at θ = 30 and 40°, along with soil moisture measurements over F3. F3_SM_MAFRI is the soil moisture measured by the MAFRI station.

6.1.2. At C-Band Using RADARSAT-2 Data at 20, 25 and 30°

In contrast to L-band, all linear and circular backscattering coefficients at C-band showed small variations with soil moisture (Figure 6). Over the F1 site, the variations in the temporal profiles are due to the difference in the incidence angles of RADARSAT-2 images (20, 25, and 30°, Table 5). However, over the F3 site, due to a high volume contribution, the sensitivity of the signal to the incidence angle decreased. At C-band, unlike what was observed at L-band, HH and VV are superimposed even over the F1 site. This is a sign of depolarization resulting from a high volume contribution at the C-band [60–62] which reduces the contribution of the interaction term [34]. The circular polarizations present different behavior than in L-band. RL is higher than RR and LL. The latter (RR and LL) are superimposed and close to HV, while RL is close to HH and VV (Figure 6). According to Baronti, et al. [60], these behaviors are mainly related to vegetation characteristics that govern the volume scattering.

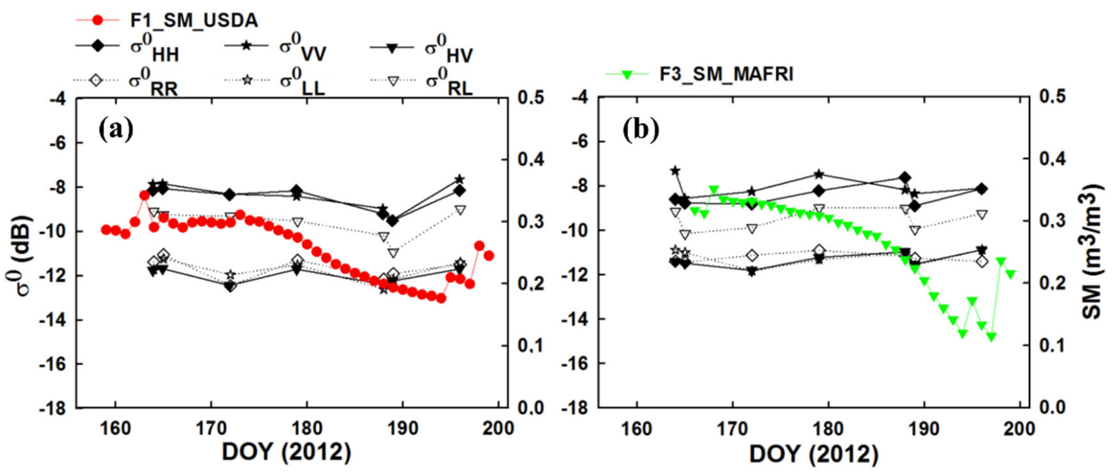

Figure 6. Temporal profile of C-band linear (HH, VV, and HV) and circular (RR, LL, and RL) polarized backscattering along with soil moisture measurements (F1_SM_USDA and F3_SM_MAFRI) over (**a**) F1 and (**b**) F3 sites.

6.2. Potential of PolSAR Parameters for Soil Moisture Retrievals over Forested Sites

6.2.1. From L- and C- bands Backscattering Coefficients

Table 7 shows the correlation coefficients between soil moisture and the L-band linear and circular backscattering coefficients acquired at 30° over F1, F2, F3, and F5 sites. In most cases, significant correlations are observed (*p*-value lower than 0.05). Compared to the results obtained over the 3 other sites, F2 presents the low correlation values and cases of non-significant correlations. This can be explained by the characteristics of the F2 site which combine high tree water content value and about 50% of mixed floor cover composed of litter and shrubs (Table 3). In addition, Table 2 shows that in the UAVSAR look direction, the F2 site presents high values of surface rms height, which will degrade the potential of soil moisture monitoring.

Table 7. Correlation coefficients of σ^0 vs. soil moisture at L-band ($\theta = 30°$) for F1, F2, F3, and F5 sites. significant correlations (*p*-value < 0.05) are denoted with '*'.

	F1	F2	F3	F5
$\sigma^0_{HH\_30°}$	0.60 *	0.50	0.62 *	0.82 *
$\sigma^0_{VV\_30°}$	0.78 *	0.77 *	0.77 *	0.96 *
$\sigma^0_{HV\_30°}$	0.80 *	0.65 *	0.85 *	0.94 *
$\sigma^0_{RR\_30°}$	0.64 *	0.56	0.66 *	0.84 *
$\sigma^0_{LL\_30°}$	0.68 *	0.64 *	0.81 *	0.88 *
$\sigma^0_{RL\_30°}$	0.69 *	0.66 *	0.70 *	0.92 *

These results are in agreement with Wang, et al. [61] who studied the sensitivity of L- and C- bands backscattering coefficients to ground surface over forested regions. The parameters of their model are the litter depth, the litter volumetric moisture, the surface roughness (rms height and correlation length), and the soil moisture. They concluded that at L-band, HH and VV acquisitions between 20 to 40° incidence angles allow the monitoring of soil moisture. At this frequency, the surface rms height acts more on the radar signal than the correlation length which almost doesn't affect the signal. Unlike our results, they showed slight sensitivity of HV polarization to soil moisture for only low forest biomass observed between 20 and 30° incidence angles. Indeed, in Table 7, at L-band, HV leads to good and significant correlations with soil moisture even over the forest with dense biomass.

Compared to L-band, the correlations of C-band RADARSAT-2 data at 20, 25, and 30° are low and not significant (Table 8) over the F1, F2, and F3, forested sites (recall that F5 is not covered with RADARSAT-2 images at the same dates as ground soil moisture measurements, Section 5.2). Therefore, the C-band backscattered signal in linear or circular polarizations is not suitable to monitor the soil moisture even over the F1 site characterized by low biomass. In accord with several authors [22,61], the low C-band signal penetration into the canopy and the volume contribution from the biomass reduce the sensitivity of the signal to soil parameters.

Table 8. Correlation coefficients of σ^0 vs. soil moisture at C-band for F1, F2, and F3 sites.

	F1	F2	F3
σ^0_{HH}	0.74	0.55	0.30
σ^0_{VV}	0.56	0.58	0.30
σ^0_{HV}	0.31	0.01	0.69
σ^0_{RR}	0.31	0.76	0.84
σ^0_{LL}	0.53	0.21	0.74
σ^0_{RL}	0.63	0.62	0.16

6.2.2. From L and C- bands Polarimetric Parameters

Freeman-Durden decomposition: Over F1, F2, F3, and F5 sites, Figure 7 shows increasing relationships between soil moisture and soil contribution (Ps) and soil-vegetation double bounce contribution (Pd) at L-band. The slope and the correlation coefficient values of these relationships decrease with the increase in forest biomass. Table 9 shows low and non-significant correlations between soil moisture and Ps over F2 and F3 sites, and between soil moisture and Pd over F3. Indeed, over forest sites with high biomass and high tree water content values (Table 3), a high volume scattering prevents Ps and Pd to monitor soil moisture.

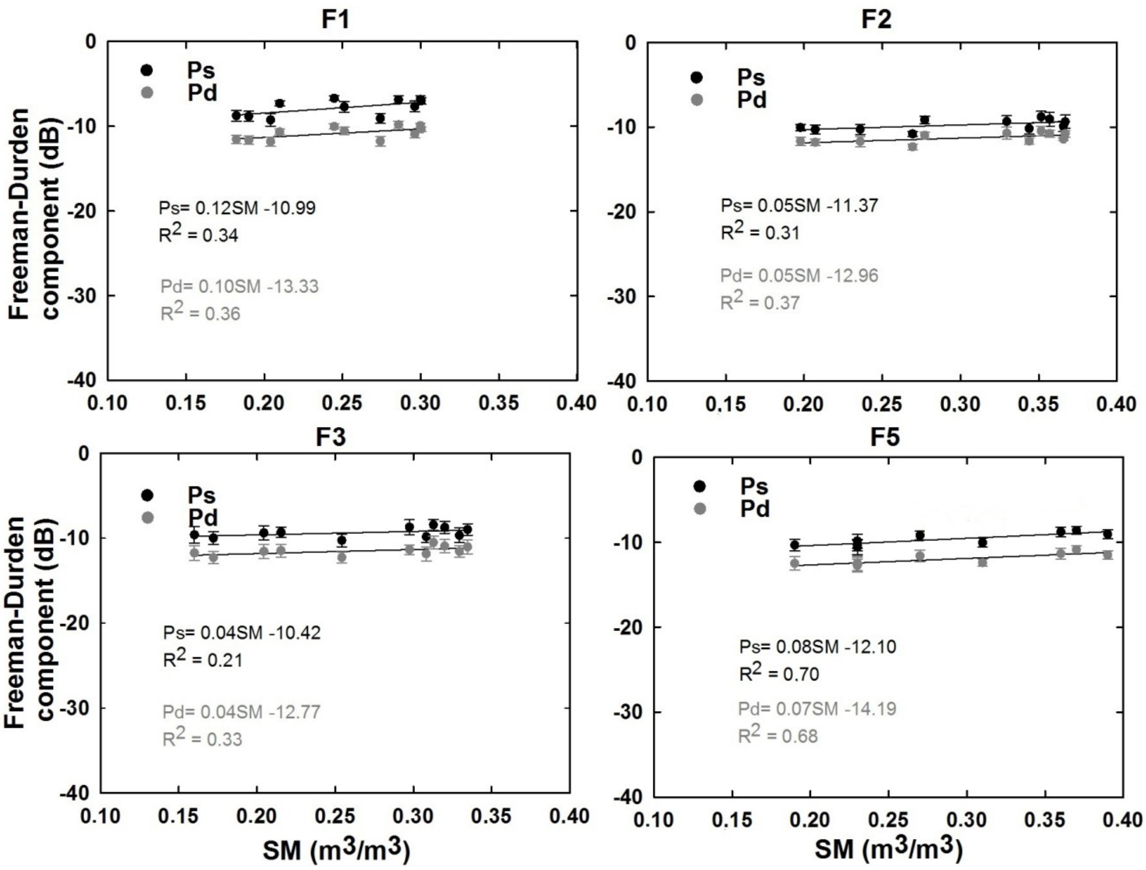

Figure 7. Relationships between the soil moisture and the mean values of Ps and Pd at L-band over F1, F2, F3, and F5 sites. The error bars represent the standard deviation of Ps and Pd within each forest site.

Table 9. Correlation coefficients between the soil moisture and the mean values of Ps and Pd at L and C- bands over F1, F2, F3, and F5 sites. Significant correlations (p-value < 0.05) are denoted with '*'.

	F1	F2	F3	F5
Ps_L_30°	**0.59 ***	0.55	0.46	**0.84 ***
Pd_L_30°	**0.60 ***	**0.61 ***	0.57	**0.82 ***
Ps_C	0.65	0.74	0.56	
Pd_C	**0.83 ***	**0.88 ***	**0.95 ***	

At C-band, while Pd presents significant correlations with soil moisture over F1, F2, and F3 sites (Table 9), Ps doesn't show any potential for soil moisture monitoring (no significant correlation). However, these C-band results should be interpreted with caution due to the limitation in the dataset used and in the distribution of soil moisture values over the sites. Indeed, two and three point clouds appear in Figure 8 for F1 and F3 sites, respectively. They are not enough to account for the high variability (standard deviation) observed in Ps and Pd over a given forested site (Figure 8).

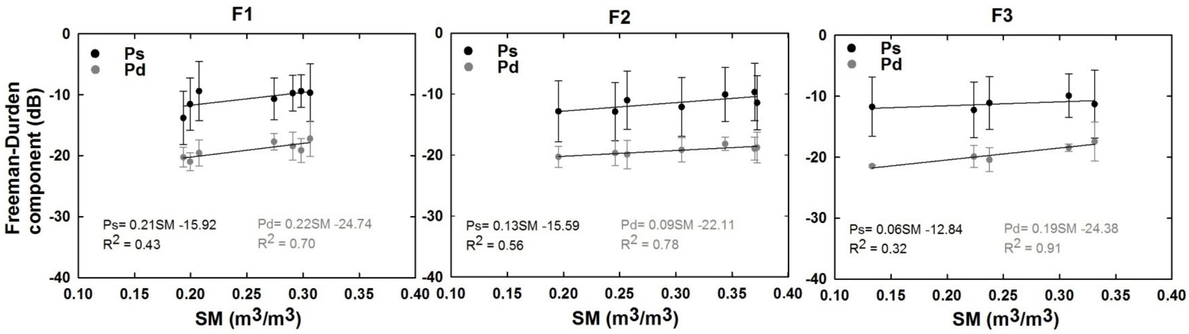

Figure 8. Relationships between the soil moisture and the mean values of Ps and Pd at C-band over F1, F2, and F3 sites. The error bars represent the standard deviation of Ps and Pd within each forest site.

Cloude–Pottier decomposition: For both L- and C- bands, Cloude-Pottier decomposition parameters (H, A, α) do not provide any significant correlation with soil moisture over all the forested sites (Table 10). In fact, in the H/α plan, the scattering mechanisms are mainly located in the volume scattering zone, leading to the low sensitivity of Cloude-Pottier parameters to soil moisture. These results are in agreement with those obtained by [17,18] over boreal forests.

Table 10. Correlation coefficients of the mean values of polarimetric parameters to the soil moisture at L-band (θ = 30°) for F1, F2, F3, and F5 sites and at C-band for F1, F2, and F3 sites. Significant correlations (p-value < 0.05) are shown with '*'.

		F1	F2	F3	F5
L-band	Pedestal Height	0.31	0.11	0.32	0.44
	ρ_{HHHV}	0.56	**0.61** *	0.57	0.02
	ρ_{VVHV}	**0.65** *	0.38	0.03	0.53
	ρ_{HHVV}	0.39	0.28	0.40	0.06
	φ_{HHHV}	0.29	0.33	**0.81** *	0.30
	φ_{VVHV}	0.03	0.46	0.25	0.06
	φ_{HHVV}	0.26	0.33	**0.60** *	0.47
	Entropy	0.35	0.14	0.29	0.48
	Alpha	0.24	0.16	0.55	0.07
	Anisotropy	0.12	0.12	0.38	0.27
C-band	Pedestal Height	0.53	0.65	0.14	
	ρ_{HHHV}	0.07	0.73	0.16	
	ρ_{VVHV}	0.15	0.33	0.15	
	ρ_{HHVV}	0.21	0.73	0.58	
	φ_{HHHV}	0.17	0.08	**0.96** *	
	φ_{VVHV}	**0.85** *	0.06	0.00	
	φ_{HHVV}	**0.90** *	0.03	**0.90** *	
	Entropy	0.39	0.69	0.14	
	Alpha	0.37	0.71	0.17	
	Anisotropy	0.68	0.01	0.30	

Pedestal height: While Bourgeau-Chavez, et al. [17] found a significant correlation (p-value < 0.05) between the pedestal height and the soil moisture, Table 10 shows that for both L- and C- bands, the pedestal height is independent of soil moisture over all the forested sites.

Correlation coefficient: In some cases, at L-band (ρ_{HHHV}_30° in F2; ρ_{VVHV}_30° in F1, φ_{HHHV}_30° and φ_{HHVV}_30° in F3) and C-band (φ_{VVHV}, φ_{HHVV} in F1 and φ_{HHHV},

φ_{HHVV} in F3), the amplitude of the correlation coefficient (ρ) and the phase (φ) showed a significant correlation with soil moisture (Table 10). However, the results in C-band should be considered with caution due to the same reason already mentioned about the limitation in the dataset used.

7. Conclusions

In this work, a comparative study was conducted to evaluate the potential of polarimetric L-band UAVSAR and C-band RADARSAT-2 data for soil moisture monitoring over SAMPVEX12 forested sites (Manitoba, Canada). Prior to data analysis, PolSAR data was processed including boxcar filtering and geometric corrections. Then the relationships between soil moisture, σ^0, and some polarimetric parameters are analyzed. Results showed that: (1) At C-band, soil moisture cannot be monitored using linear or circular backscattering coefficients over SMAPVEX12 forested sites even for the low-biomass site. At L-band, linear or circular backscattering coefficients were in most cases significantly correlated to soil moisture over the forested sites. Therefore, with respect to the C-band, this comparative study confirmed the higher potential of the L-band linear and circular backscattering coefficients for soil moisture monitoring over forested sites. (2) While at L-band ($\theta = 30°$) Ps and Pd showed great potential for soil moisture monitoring over the less dense forested sites (F1 and F5), at the C-band the observed weak potential of Ps and the high potential of Pd should be interpreted with caution due to the limitation in the dataset used and in the distribution of soil moisture values over the sites. (3) For both C- and L-bands, Cloude-Pottier decomposition parameters (H, A, and α) and the pedestal height show no potential for soil moisture monitoring over SMAPVEX12 forested sites. (4) For the amplitude and the phase of the correlation coefficient, in some cases, they give significant correlations with soil moisture for both L- and C- bands. At C-band, the dataset used showed significant relationships between some polarimetric parameters (φ_{VVHV}, φ_{HHVV} in F1 and φ_{HHVV}, φ_{HHHV} in F3) and soil moisture.

Compared to σ^0, the C-band polarimetric parameters provided an added value for soil moisture monitoring. This result is interesting since σ^0 at the C-band saturates quickly over forested areas. Although the phases (φ_{HHHV}, φ_{VVHV}, and φ_{HHVV}) of the correlation coefficients between multi-polarized channels are found to be significantly correlated to soil moisture (r~0.90), the developed relationships at C-band must be tested over others sites and other datasets. However, compared to σ^0, the results obtained with the L-band polarimetric parameters did not show any additional or significant contributions to soil moisture monitoring. Based on the results obtained in this study, future works will be devoted to the development of empirical soil moisture retrieval models for forested sites, using the identified optimal PolSAR parameters (backscattering coefficients and polarimetric parameters most strongly correlated with soil moisture).

Author Contributions: Conceptualization, R.M. and K.G.; methodology, S.J. and R.M.; software, S.J.; validation, S.J., R.M., H.W., K.G. and A.C.; formal analysis, S.J. and H.W.; writing—original draft preparation, S.J., R.M. and H.W.; writing—review and editing, R.M., H.W. and A.C.; supervision, R.M. and K.G.; funding acquisition, R.M. and K.G. All authors have read and agreed to the published version of the manuscript.

Funding: This study was funded by the Canadian Space Agency Class Grant and the Contribution Program (11SUSMAPSH) as part of the Canadian plan for spatial missions of soil moisture and the National Science and Engineering Research Council of Canada (RGPIN 283211-2011).

Data Availability Statement: The SMAPVEX12-MB datasets reported in this paper can be accessed through: https://smapvex12.espaceweb.usherbrooke.ca (accessed on 17 October 2022).

Acknowledgments: The authors would like to thank the funding agencies (NSERC, EC, CSA, AAFC, NASA, USDA) of the SMAPVEX12 campaign and all the participants to this campaign. A contribution to this work was made at Jet Propulsion Laboratory, California Institute of Technology under a contract with National Aeronautics and Space Administration.

Conflicts of Interest: The authors declare no conflict of interest.

References

1. Sokol, J.; NcNairn, H.; Pultz, T.J. Case studies demonstrating the hydrological applications of C-band multipolarized and polarimetric SAR. *Can. J. Remote Sens.* **2004**, *30*, 470–483. [CrossRef]
2. Kirkby, M. Modelling the interactions between soil surface properties and water erosion. *CATENA* **2002**, *46*, 89–102. [CrossRef]
3. Römkens, M.; Helming, K.; Prasad, S. Soil erosion under different rainfall intensities, surface roughness, and soil water regimes. *CATENA* **2002**, *46*, 103–123. [CrossRef]
4. Ziadat, F.M.; Taimeh, A.Y. Effect of rainfall intensity, slope, land use and antecedent soil moisture on soil erosion in an arid environment. *Land Degrad. Dev.* **2013**, *24*, 582–590. [CrossRef]
5. Entekhabi, D.; Njoku, E.G.; Neill, P.E.O.; Kellogg, K.H.; Crow, W.T.; Edelstein, W.N.; Entin, J.K.; Goodman, S.D.; Jackson, T.J.; Johnson, J.; et al. The Soil Moisture Active Passive (SMAP) Mission. *Proc. IEEE* **2010**, *98*, 704–716. [CrossRef]
6. WMO. *ECV Products and Requirements for Soil Moisture*; World Meteorological Organization: Geneva, Switzerland, 2008.
7. Lavoie, M.; Paré, D.; Fenton, N.; Groot, A.; Taylor, K. Paludification and management of forested peatlands in Canada: A literature review. *Environ. Rev.* **2005**, *13*, 21–50. [CrossRef]
8. Bourgeau-Chavez, L.L.; Garwood, G.; Riordan, K.; Cella, B.; Alden, S.; Kwart, M.; Murphy, K. Improving the prediction of wildfire potential in boreal Alaska with satellite imaging radar. *Polar Rec.* **2007**, *43*, 321–330. [CrossRef]
9. Kurum, M.; O'Neill, P.E.; Lang, R.H.; Joseph, A.T.; Cosh, M.H.; Jackson, T.J. Effective tree scattering and opacity at L-band. *Remote Sens. Environ.* **2012**, *118*, 1–9. [CrossRef]
10. Colliander, A.; Cosh, M.H.; Kelly, V.R.; Kraatz, S.; Bourgeau-Chavez, L.; Siqueira, P.; Roy, A.; Konings, A.G.; Holtzman, N.; Misra, S.; et al. SMAP Detects Soil Moisture Under Temperate Forest Canopies. *Geophys. Res. Lett.* **2020**, *47*, e2020GL089697. [CrossRef]
11. Colliander, A.; Njoku, E.G.; Huang, H.; Tsang, L. Soil Moisture Retrieval Using full Wave Simulations of 3-D Maxwell Equations for Compensating Vegetation Effects. In Proceedings of the IEEE International Geoscience and Remote Sensing Symposium, Valencia, Spain, 22–27 July 2018; pp. 1418–1421.
12. Colliander, A.; Cosh, M.H.; Berg, A.; Misra, S.; Thomas, J.; Bourgeau-Chavez, L.; Kelly, V.; Kraatz, S.; Siqueira, P.; Roy, A.; et al. Development of SMAP Retrievals for Forested Regions: SMAPVEX19-22 and SMAPVEX22-Boreal. In Proceedings of the IEEE International Geoscience and Remote Sensing Symposium, Kuala Lumpur, Malaysia, 17–22 July 2022; pp. 4228–4231.
13. Das, N.N.; Entekhabi, D.; Dunbar, R.S.; Chaubell, M.J.; Colliander, A.; Yueh, S.; Jagdhuber, T.; Chen, F.; Crow, W.; O'Neill, P.E.; et al. The SMAP and Copernicus Sentinel 1A/B microwave active-passive high resolution surface soil moisture product. *Remote Sens. Environ.* **2019**, *233*, 111380. [CrossRef]
14. Das, N.N.; Entekhabi, D.; Dunbar, R.S.; Colliander, A.; Chen, F.; Crow, W.; Jackson, T.J.; Berg, A.; Bosch, D.D.; Caldwell, T.; et al. The SMAP mission combined active-passive soil moisture product at 9 km and 3 km spatial resolutions. *Remote Sens. Environ.* **2018**, *211*, 204–217. [CrossRef]
15. Ferrazzoli, P.; Guerriero, L. Radar sensitivity to tree geometry and woody volume: A model analysis. *IEEE Trans. Geosci. Remote Sens.* **1995**, *33*, 360–371. [CrossRef]
16. Pulliainen, J.T.; Mikhela, P.J.; Hallikainen, M.T.; Ikonen, J. Seasonal dynamics of C-band backscatter of boreal forests with applications to biomass and soil moisture estimation. *IEEE Trans. Geosci. Remote Sens.* **1996**, *34*, 758–770. [CrossRef]
17. Bourgeau-Chavez, L.; Leblon, B.; Charbonneau, F.; Buckley, J.R. Assessment of polarimetric SAR data for discrimination between wet versus dry soil moisture conditions. *Int. J. Remote Sens.* **2013**, *34*, 5709–5730. [CrossRef]
18. Bourgeau-Chavez, L.; Leblon, B.; Charbonneau, F.; Buckley, J. Evaluation of polarimetric Radarsat-2 SAR data for development of soil moisture retrieval algorithms over a chronosequence of black spruce boreal forests. *Remote Sens. Environ.* **2013**, *132*, 71–85. [CrossRef]
19. Wagner, W.; Blöschl, G.; Pampaloni, P.; Calvet, J.-C.; Bizzarri, B.; Wigneron, J.-P.; Kerr, Y. Operational readiness of microwave remote sensing of soil moisture for hydrologic applications. *Hydrol. Res.* **2007**, *38*, 1–20. [CrossRef]
20. Jagdhuber, T.; Hajnsek, I.; Sauer, S.; Papathanassiou, K.P.; Bronstert, A. Soil moisture retrieval under forest using polarimetric decomposition techniques at P-band. In Proceedings of the 9th European Conference on Synthetic Aperture Radar, Nuremberg, Germany, 23–26 April 2012; pp. 709–712.
21. Kurum, M.; Kim, S.B.; Akbar, R.; Cosh, M.H. Surface Soil Moisture Retrievals Under Forest Canopy for L-Band SAR Observations Across a Wide Range of Incidence Angles by Inverting a Physical Scattering Model. *IEEE J. Sel. Top. Appl. Earth Obs. Remote Sens.* **2021**, *14*, 1741–1753. [CrossRef]
22. Freeman, A.; Durden, S.L. A three-component scattering model for polarimetric SAR data. *IEEE Trans. Geosci. Remote Sens.* **1998**, *36*, 963–973. [CrossRef]
23. Mitchard, E.T.A.; Saatchi, S.S.; Woodhouse, I.H.; Nangendo, G.; Ribeiro, N.S.; Williams, M.; Ryan, C.M.; Lewis, S.L.; Feldpausch, T.R.; Meir, P. Using satellite radar backscatter to predict above-ground woody biomass: A consistent relationship across four different African landscapes. *Geophys. Res. Lett.* **2009**, *36*, L23401. [CrossRef]
24. Pulliainen, J.; Hari, P.; Hallikainen, M.; Patrikainen, N.; Peramaki, M.; Kolari, P. Monitoring of soil moisture and vegetation water content variations in boreal forest from C-band SAR data. In Proceedings of the IEEE International Geoscience and Remote Sensing Symposium, Anchorage, AK, USA, 20–24 September 2004; pp. 1013–1016.

25. Abbott, K.N.; Leblon, B.; Staples, G.C.; Maclean, D.A.; Alexander, M.E. Fire danger monitoring using RADARSAT-1 over northern boreal forests. *Int. J. Remote Sens.* **2007**, *28*, 1317–1338. [CrossRef]
26. Tabatabaeenejad, A.; Burgin, M.; Moghaddam, M. Potential of L-Band Radar for Retrieval of Canopy and Subcanopy Parameters of Boreal Forests. *IEEE Trans. Geosci. Remote Sens.* **2012**, *50*, 2150–2160. [CrossRef]
27. Touzi, R.; Goze, S.; Toan, T.L.; Lopes, A.; Mougin, E. Polarimetric discriminators for SAR images. *IEEE Trans. Geosci. Remote Sens.* **1992**, *30*, 973–980. [CrossRef]
28. McNairn, H.; Brisco, B. The application of C-band polarimetric SAR for agriculture: A review. *Can. J. Remote Sens.* **2004**, *30*, 525–542. [CrossRef]
29. Cloude, S.R.; Pottier, E. An entropy based classification scheme for land applications of polarimetric SAR. *IEEE Trans. Geosci. Remote Sens.* **1997**, *35*, 68–78. [CrossRef]
30. Touzi, R.; Deschamps, A.; Rother, G. Wetland characterization using polarimetric RADARSAT-2 capability. *Can. J. Remote Sens.* **2007**, *33*, S56–S67. [CrossRef]
31. van Zyl, J.J.; Arii, M.; Kim, Y. Model-based decomposition of polarimetric SAR covariance matrices constrained for nonnegative eigenvalues. *IEEE Trans. Geosci. Remote Sens.* **2011**, *49*, 3452–3459. [CrossRef]
32. Lee, J.S.; Pottier, E. *Polarimetric Radar Imaging from Basics to Applications*; CRC Press: Boca Raton, FL, USA, 2009.
33. Moghaddam, M.; Saatchi, S.; Cuenca, R. Estimating subcanopy soil moisture with radar. *J. Geophys. Res.* **2000**, *105*, 14899–14912. [CrossRef]
34. Fung, A.K. *Microwave Scattering and Emission Models and Their Applications*; Artech House Signal Processing Library: Norwood, MA, USA, 1994.
35. Harrell, P.A.; Bourgeau-Chavez, L.L.; Kasischke, E.S.; French, N.H.F.; Christensen, N.L.J.R.S.o.E. Sensitivity of ERS-1 and JERS-1 radar data to biomass and stand structure in Alaskan boreal forest. *Remote Sens. Environ.* **1995**, *54*, 247–260. [CrossRef]
36. Truong-Loï, M.; Saatchi, S.; Jaruwatanadilok, S. Soil Moisture Estimation Under Tropical Forests Using UHF Radar Polarimetry. *IEEE Trans. Geosci. Remote Sens.* **2015**, *53*, 1718–1727. [CrossRef]
37. Moghaddam, M.; Saatchi, S. Analysis of scattering mechanisms in SAR imagery over boreal forest: Results from BOREAS '93. *IEEE Trans. Geosci. Remote Sens.* **1995**, *33*, 1290–1296. [CrossRef]
38. Magagi, R.; Berg, A.A.; Goita, K.; Belair, S.; Jackson, T.J.; Toth, B.; Walker, A.; McNairn, H.; Neill, P.E.O.; Moghaddam, M.; et al. Canadian Experiment for Soil Moisture in 2010 (CanEx-SM10): Overview and Preliminary Results. *IEEE Trans. Geosci. Remote Sens.* **2013**, *51*, 347–363. [CrossRef]
39. Said, S.; Kothyari, U.C.; Arora, M.K. Vegetation effects on soil moisture estimation from ERS-2 SAR images. *Hydrol. Sci. J.* **2012**, *57*, 517–534. [CrossRef]
40. Hajnsek, I.; Jagdhuber, T.; Schon, H.; Papathanassiou, K.P. Potential of estimating soil moisture under vegetation cover by means of PolSAR. *IEEE Trans. Geosci. Remote Sens.* **2009**, *47*, 442–454. [CrossRef]
41. Baghdadi, N.; Cresson, R.; Pottier, E.; Aubert, M.; Zribi, M.; Jacome, A.; Benabdallah, S. A potential use for the C-band polarimetric SAR parameters to characterize the soil surface over bare agriculture fields. *IEEE Trans. Geosci. Remote Sens.* **2012**, *50*, 3844–3858. [CrossRef]
42. Baghdadi, N.; Dubois-Fernandez, P.; Dupuis, X.; Zribi, M. Sensitivity of Main Polarimetric Parameters of Multifrequency Polarimetric SAR Data to Soil Moisture and Surface Roughness Over Bare Agricultural Soils. *IEEE Geosci. Remote Sens. Lett.* **2013**, *10*, 731–735. [CrossRef]
43. Jagdhuber, T.; Hajnsek, I.; Bronstert, A.; Papathanassiou, K.P. Soil moisture estimation under low vegetation cover using a multi-angular polarimetric decomposition. *IEEE Trans. Geosci. Remote Sens.* **2013**, *51*, 2201–2215. [CrossRef]
44. Wang, H.; Magagi, R.; Goita, K. Comparison of different polarimetric decompositions for soil moisture retrieval over vegetation covered agricultural area. *Remote Sens. Environ.* **2017**, *199*, 120–136. [CrossRef]
45. Toan, T.L.; Beaudoin, A.; Riom, J.; Guyon, D. Relating forest biomass to SAR data. *IEEE Trans. Geosci. Remote Sens.* **1992**, *30*, 403–411. [CrossRef]
46. Borgeaud, M.; Noll, J. Analysis of theoretical surface scattering models for polarimetric microwave remote sensing of bare soils. *Int. J. Remote Sens.* **1994**, *15*, 2931–2942. [CrossRef]
47. Skriver, H.; Svendsen, M.T.; Thomsen, A.G. Multitemporal C- and L-band polarimetric signatures of crops. *IEEE Trans. Geosci. Remote Sens.* **1999**, *37*, 2413–2429. [CrossRef]
48. McNairn, H.; Ellis, J.; Sanden, V.D.; Hirose, T.; Brown, R.J. Providing crop information using RADARSAT-1 and satellite optical imagery. *Int. J. Remote Sens.* **2002**, *23*, 851–870. [CrossRef]
49. Adams, J.R.; Bergand, A.A.; McNairn, H.; Merzouki, A. Sensitivity of C-band SAR polarimetric variables to unvegetated agricultural fields. *Can. J. Remote Sens.* **2013**, *39*, 1–16. [CrossRef]
50. Mattia, F.; Le Toan, T.; Souyrb, J.; De Carolis, G.; Floury, N.; Posa, F.; Pasquariello, G. The effect of surface roughness on multifrequency polarimetric SAR data. *IEEE Trans. Geosci. Remote Sens.* **1997**, *35*, 954–966. [CrossRef]
51. Wang, H.; Magagi, R.; Goita, K.; Jagdhuber, T.; Hajnsek, I. Evaluation of simplified polarimetric decomposition for soil moisture retrieval over vegetated agricultural fields. *Remote Sens.* **2016**, *8*, 142. [CrossRef]
52. Hajnsek, I.; Pottier, E.; Cloude, S.R. Inversion of surface parameters from polarimetric SAR. *IEEE Trans. Geosci. Remote Sens.* **2003**, *41*, 727–744. [CrossRef]

53. Allain, S.; Ferro-Famil, L.; Pottier, E.; Hajnsek, I. Extraction of surface parameters from multi-frequency and polarimetric SAR data. In Proceedings of the IEEE International Geosicence and Remote Sensing Symposium, Kuala Lumpur, Malaysia, 17–22 July 2022; pp. 426–428.
54. Gonçalves, F.G.; Santos, J.R.; Treuhaft, R.N. Stem volume of tropical forests from polarimetric radar. *Int. J. Remote Sens.* **2011**, *32*, 503–522. [CrossRef]
55. Jagdhuber, T.; Hajnsek, I.; Papathanassiou, K.P. An iterative generalized hybrid decomposition for soil moisture retrieval under vegetation cover using fully polarimetric SAR. *IEEE J. Sel. Top. Appl. Earth Obs. Remote Sens.* **2015**, *8*, 3911–3922. [CrossRef]
56. McNairn, H.; Jackson, T.J.; Wiseman, G.; Belair, S.; Berg, A.; Bullock, P.; Colliander, A.; Cosh, M.H.; Kim, S.-B.; Magagi, R.; et al. The Soil Moisture Active Passive Validation Experiment 2012 (SMAPVEX12): Prelaunch calibration and validation of the SMAP soil moisture algorithms. *IEEE Trans. Geosci. Remote Sens.* **2015**, *53*, 2784–2801. [CrossRef]
57. Lambert, M.-C.; Ung, C.-H.; Raulier, F. Canadian national tree aboveground biomass equations. *Can. J. For. Res.* **2005**, *35*, 1996–2018. [CrossRef]
58. Lee, J.; Ainsworth, T.L.; Kelly, J.P.; Lopez-Martinez, C. Evaluation and Bias Removal of Multilook Effect on Entropy/Alpha/Anisotropy in Polarimetric SAR Decomposition. *IEEE Trans. Geosci. Remote Sens.* **2008**, *46*, 3039–3052. [CrossRef]
59. López-Martínez, C.; Alonso-González, A.; Fàbregas, X. Perturbation Analysis of Eigenvector-Based Target Decomposition Theorems in Radar Polarimetry. *IEEE Trans. Geosci. Remote Sens.* **2014**, *52*, 2081–2095. [CrossRef]
60. Baronti, S.; Del Frate, F.; Ferrazzoli, P.; Paloscia, S.; Pampaloni, P.; Schiavon, G. SAR polarimetric features of agricultural areas. *Int. J. Remote Sens.* **1995**, *16*, 2639–2656. [CrossRef]
61. Wang, Y.; Day, J.L.; Davis, F.W. Sensitivity of Modeled C- and L-Band Radar Backscatter to Ground Surface Parameters in Loblolly Pine Forest. *Remote Sens. Environ.* **1998**, *66*, 331–342. [CrossRef]
62. Cable, J.W.; Kovacs, J.M.; Shang, J.; Jiao, X. Multi-Temporal Polarimetric RADARSAT-2 for Land Cover Monitoring in Northeastern Ontario, Canada. *Remote Sens.* **2014**, *6*, 2372–2392. [CrossRef]